EFFECT OF THE DISTRIBUTION OF THE ELEMENTS IN A CAPACITIVE ENERGY STORE ON THE NATURE OF THE PLASMA CURRENT IN A COAXIAL CHANNEL

N. V. Belan, L. P. Kovalevskaya, and N. A. Mashtylev

UDC 533.95:538.4

When investigating magnetohydrodynamic flows it was found [1-4] that there is a complex relationship between the plasma parameters and the experimental conditions and properties of the flows being investigated. A mathematical simulation of the steady-state flow of a plasma in coaxial channels [5, 6] enabled the features of the dynamics of the flows to be established and enabled an analysis of the flow pattern as a function of the plasma parameters to be made. It was shown that after a certain time interval corresponding to the transient time, time-invariant plasma parameters, which also determine other forms of the flow are established at each point of the channel. When analyzing non-steady-state plasma acceleration [7-9], a nonuniform distribution of the parameters both in space and in time was found. One of the reasons for the complex magnetohydrodynamic flow pattern of a plasma is the dependence of the flow parameters and the electromagnetic field on the constructional features of the energy store.

In this paper, using the two-dimensional MHD approximation (edge effects are ignored), the results of calculations of the effect of the distribution of the RLC sections of the capacitive energy store on the nature of the plasma flow in a coaxial channel are presented.

A capacitive energy store consists of an RLC sections. This enables one, by changing the number of RLC sections while keeping the capacitance of the capacitor battery constant, to obtain both non-steady-state plasma flow, when the characteristic time of the variation of the processes in the electric circuit is much less than the transit time of the plasma in the channel, and steady-state flows with the opposite time relations.

The equivalent electric circuit of a plasma injector with a capacitive energy store is shown in Fig. 1, where 1 is the supply source; 2 is the coaxial accelerator; 3 is the capacitive energy store consisting of an RLC sections; C_k, L_k, and R_k are the capacitance, inductance, and resistance, respectively, of the k-th section; and I_k^c and I_k are the currents in the capacitances and inductances of the k-th section.

Considering the flow of a nonviscous plasma with constant transfer coefficients, and neglecting the Hall effect in the induction equation, we will write the system of magnetohydrodynamic equations in the form

$$\begin{gathered}
\partial\rho/\partial t + \operatorname{div}\rho\mathbf{v} = 0,\\
\partial\mathbf{v}/\partial t + (\mathbf{v}\nabla)\mathbf{v} = -(1/\rho)\nabla p + (1/\mu\rho)[\operatorname{rot}\mathbf{B},\mathbf{B}],\\
p = (2\rho/M)kT,\\
C_V\rho\partial T/\partial t + C_V\rho(\mathbf{v}\nabla)T = \varkappa\Delta T + (\nu_m/\mu)([\nabla\mathbf{B}])^2 - p(\nabla\mathbf{v}),\\
\partial\mathbf{B}/\partial t = \operatorname{rot}[\mathbf{v}\mathbf{B}] + \nu_m\Delta\mathbf{B},
\end{gathered} \tag{1}$$

where ρ and $\mathbf{v}$ are the density and velocity of the plasma, respectively; p is the plasma pressure; $\mathbf{B}$ is the magnetic induction; T is the plasma temperature; μ is the magnetic permeability; k is Boltzmann's constant; C_V is the specific heat of the plasma at constant volume; $\nu_m = 1/\mu\sigma$ is the magnetic viscosity; $\varkappa$ is the thermal conductivity; and M is the mass of an ion.

When solving the system of equations (1), we will use the following boundary and initial conditions: at the channel input,

$$\rho = \rho_0,\ \mathbf{v} = \mathbf{v}_0,\ T = T_0,\ \mathbf{B} = \mu I_1/2\pi r; \tag{2}$$

on the electrodes,

$$\mathbf{v}_r = 0,\ E_\tau = 0,\ T = T_0; \tag{2}$$

Khar'Kov. Translated from Zhurnal Prikladnoi Mekhaniki i Tekhnicheskoi Fiziki, No. 3, pp. 30-37, May-June, 1978. Original article submitted May 10, 1977.

0021-8944/78/1903-0303$07.50

at the channel output,

$$\mathbf{B} = 0, \ \partial T/\partial z = 0; \tag{2}$$

and at the initial instant of time,

$$\rho = \rho_0, \ \mathbf{v} = \mathbf{v}_0, \ T = T_0, \ \mathbf{B} = 0, \tag{2}$$

where $\mathbf{v}_r$ is the normal component of the velocity to the surface of the electrodes, and E_τ is the component of the electric field tangent to the surface of the electrodes.

It follows from the boundary conditions (2) that the magnetic induction at the channel input is uniquely defined by the current flowing in the accelerator. To find the value of this current we will use Kirchhoff's laws for the nodal currents (see Fig. 1):

$$\begin{gathered} C_1 dU_1/dt = I_2 - I_1, \\ \cdots \\ C_k dU_k/dt = I_{k+1} - I_k, \\ \cdots \\ C_n dU_n/dt = -I_n \end{gathered} \tag{3}$$

and the voltages in the loops of the energy store:

$$\begin{gathered} d/dt(L_1 I_1) + R_1 I_1 = U_1 - U_e, \\ \cdots \\ d/dt(L_k I_k) + R_k I_k = U_k - U_{k-1}, \\ \cdots \\ d/dt(L_n I_n) + R_n I_n = U_n - U_{n-1}, \end{gathered} \tag{4}$$

where U_e is the voltage drop across the plasma gap.

Using the laws of conservation of electromagnetic energy in the circuit

$$\sum_{k=1}^{n} \frac{C_k (U_{0k}^2 - U_k^2)}{2} = \sum_{k=1}^{n} \frac{L_k I_k^2}{2} + \sum_{k=1}^{n} \int_0^t R_k I_k^2 dt - \frac{1}{\mu} \int_0^t \oint_S [\mathbf{EB}] \, d\mathbf{S},$$

we find the voltage drop across the plasma gap:

$$U_e = -\frac{1}{\mu I_1} \oint_S [\mathbf{EB}] \, d\mathbf{S}, \tag{5}$$

where S is a closed surface bounding the volume of the accelerating chamber, and I_1 is the current in the accelerating chamber.

When the plasma is accelerated between coaxial electrodes of constant radius, Eq. (5) takes the form

$$U_e = -\frac{1}{\mu\sigma} \int_{r_1}^{r_2} \frac{\partial B(t, r, 0)}{\partial z} + \frac{\mu I_1 v_z(t, r, 0)}{2\pi} \ln \frac{r_2}{r_1}.$$

Multiplying the equations with index k in system (4) by I_{k+1}, and the equation with index k+1 by L_k, combining them in pairs, and using the fact that $I_k = -\sum_{j=k}^{n} C_j \frac{dU_j}{dt}$, Eqs. (3) and (4) become

$$\begin{gathered} \frac{d^2 U_1}{dt^2} = \left(U_2 - U_1 + R_2 \sum_{j=2}^{n} C_j \frac{dU_j}{dt}\right) \frac{1}{C_1 L_2} - \left(U_1 - U_e + R_1 \sum_{j=1}^{n} C_j \frac{dU_j}{dt}\right) \frac{1}{C_1 L_1}, \\ \cdots \\ \frac{d^2 U_k}{dt^2} = \left(U_{k+1} - U_k + R_{k+1} \sum_{j=k+1}^{n} C_j \frac{dU_j}{dt}\right) \frac{1}{C_k L_{k+1}} - \left(U_k - U_{k-1} + R_k \sum_{j=k}^{n} C_j \frac{dU_j}{dt}\right) \frac{1}{C_k L_k}, \\ \cdots \\ \frac{d^2 U_n}{dt^2} = -\left(U_n - U_{n-1} + R_n C_n \frac{dU_n}{dt}\right) \frac{1}{C_n L_n}. \end{gathered} \tag{6}$$

For convenience in investigating the processes occurring in the accelerating chamber and in the capacitive energy store, we will use dimensionless variables by dividing the required values by the characteristic values: ρ_0 and T_0 are the density and temperature of the plasma at the input to the accelerating channel; U_0 is the voltage on the capacitor battery at the initial instant of time; l_0 is the length of the channel; C_0 and L_0 are the capacitance and inductance of the circuit for n = 1; $v_0 = B_0/\sqrt{\mu\rho_0}$, $B_0 = \mu I_0/2\pi r_1$, $I_0 = U_0\sqrt{C_0/L_0}$, $p_0 = R\rho_0 T_0$, $t_0 = r_0/v_0$.

Preserving the notation, we will consider axisymmetrical flow of a plasma between coaxial electrodes of constant cross section in a cylindrical system of coordinates (r, φ, z) by representing the system of equations (1) and the boundary and initial conditions (2) in dimensionless variables

$$\begin{gathered}
\partial\rho/\partial\tau + v_r\partial\rho/\partial r + v_z\partial\rho/\partial z + \rho/r\partial/\partial r(rv_r) + \rho\partial v_z/\partial z = 0,\\
\rho\partial v_z/\partial\tau + \rho v_z\partial v_z/\partial z + \rho v_r\partial v_z/\partial r = -\beta\partial p/\partial z - 0{,}5\partial B^2/\partial z,\\
\rho\partial v_r/\partial\tau + \rho v_r\partial v_r/\partial r + \rho v_z\partial v_r/\partial z = -\beta\partial p/\partial r - 0{,}5\partial B^2/\partial r - B^2/r,\\
p = \rho T,\\
\partial T/\partial\tau + v_z\partial T/\partial z + v_r\partial T/\partial r = 1/\Pi\rho\cdot\partial^2 T/\partial z^2 + (1/\Pi\rho r)\partial/\partial r\cdot(r\partial T/\partial r) -\\
-\beta\varepsilon T\partial v_z/\partial z - \beta\varepsilon T\left[\left(\frac{1}{r}\right)\partial/\partial r\cdot(rv_r)\right] + \varepsilon\eta\,[(1/\rho)\cdot(\partial B/\partial z)^2] + \varepsilon\eta\,(1/\rho)\,[(1/r)\,\partial/\partial r\cdot(rB)]^2,\\
\partial B/\partial\tau = \eta\partial^2 B/\partial z^2 + \eta\partial/\partial r[(1/r)\partial/\partial r\cdot(rB)] - v_z\partial B/\partial z - v_r\partial B/\partial z - B\partial v_z/\partial z - B\partial v_r/\partial r;
\end{gathered} \tag{7}$$

$$\begin{gathered}
\text{for } \tau = 0\text{: } \rho = 1,\ v_z = 0{,}1,\ v_r = 0,\ T = 1,\ B = 0;\\
\text{for } z = 0\text{: } \rho = 1,\ v_z = 0,\ 1,\ v_r = 0,\ T = 1,\ B = -N_1N_3\frac{\sum_{j=1}^{n} A_j\frac{dU_j}{d\tau}}{r};\\
\text{for } r = r_1 \text{ and } r = r_2,\ v_r = 0,\ E_\tau = 0,\ T = 1;\\
\text{for } z = 1\text{: } B = 0,\ \partial T/\partial z = 0.
\end{gathered} \tag{8}$$

The quantity $\sum_{j=1}^{n} A_j\frac{dU_j}{d\tau}$ is found from the system of equations (6) written in the dimensionless variables

$$\begin{aligned}
\frac{d^2U_1}{d\tau^2} &= \left(U_2 - U_1 + N_2D_2\sum_{j=2}^{n} A_j\frac{dU_j}{d\tau}\right)\frac{1}{N_3^2A_1B_2} -\\
&-\left(U_1 + \frac{\delta}{N_1}\int_{r_1}^{r_2}\frac{\partial B(\tau, r, 0)}{\partial z}dr + \frac{\delta N_3}{\eta N_1}\ln\frac{r_2}{r_1}\sum_{j=1}^{n} A_j\frac{dU_j}{d\tau} +\right.\\
&\left. + N_2D_1\sum_{j=1}^{n} A_j\frac{dU_j}{d\tau}\right)\frac{1}{N_3^2A_1B_1},\\
&\cdots\\
\frac{d^2U_k}{d\tau^2} &= \left(U_{k+1} - U_k + N_2D_{k+1}\sum_{j=k+1}^{n} A_j\frac{dU_j}{d\tau}\right)\frac{1}{N_3^2A_kB_{k+1}}\\
&-\left(U_k - U_{k-1} + N_2D_k\sum_{j=k}^{n} A_j\frac{dU_j}{d\tau}\right)\frac{1}{N_3^2A_kB_k},\\
&\cdots\\
\frac{d^2U_n}{d\tau^2} &= -\left(U_n - U_{n-1} + N_2D_nA_n\frac{dU_n}{d\tau}\right)\frac{1}{N_3^2A_nB_n}
\end{aligned} \tag{9}$$

with initial conditions

$$U_k = 1,\ dU_k/d\tau = 0. \tag{10}$$

The dimensionless combinations are found from the expressions

$$\beta = \frac{\mu p_0}{B_0^2},\ \eta = \frac{1}{\mu\sigma l_0 v_0},\ \Pi = \frac{C_V\rho_0 l_0 v_0}{\varkappa},$$

$$\varepsilon = \frac{v_0^2}{C_V T_0},\ N_1 = \frac{r_1}{l_0},\ N_2 = \frac{R_0 C_0}{t_0},\ N_3 = \frac{\sqrt{L_0 C_0}}{t_0},$$

$$\delta = (1/2\pi l_0 \sigma)\sqrt{C_0/L_0},\ A_k = C_k/C_0,\ B_k = L_k/L_0,\ D_k = R_k/R_0.$$

The continuous solution of the system of equations (7) with initial and boundary conditions (8)-(10) was found numerically [5] in a rectangle representing the cross section of the accelerating channel normal to the surface of the electrodes after a time interval at the end of which the energy remaining in the store is approximately 1% of the energy in the store at the initial instant of time.

The problem was solved in the following order: using the Runge–Kutta method [10], we integrated the system of equations (9) with initial conditions (10) for the known distribution of the parameters of the plasma in the accelerating chamber and we determined the magnetic induction at the input of the accelerating chamber; then, using the method of finite differences, we integrated the system of equations (7) with initial and boundary conditions (8). The time step was determined from the requirement for the chosen scheme to be stable:

$$h_\tau \leqslant \frac{\min(h_r, h_z)}{\max[v + \sqrt{(\beta p + B^2)/\rho}]},$$

where h_τ, h_r, h_z are the steps in time, radius, and channel length, respectively.

As a result of the solution of the problem with varying dimensionless complexes of the system of equations and number of RLC sections in the energy store, we obtained both the non-steady-state flow modes, when before the discharge of the capacitor battery has ended the plasma bunches have not yet left the accelerator, and the quasistationary flow modes, in which an increment in the velocity occurs over the whole length of the channel and the value of the plasma velocity reaches the maximum value at the output of the accelerating channel.

To illustrate the results obtained, consider several characteristic flow modes. Figures 2-4 show the variations in the magnetic induction, density, and plasma velocity in the accelerating chamber at the instant of time $\tau = 2$ for n = 11 (Fig. 2a, 3a, and 4a), n = 7 (Figs. 2b, 3b, and 4b), and n = 1 (Figs. 2c, 3c, and 4c) for the following values of the dimensionless parameters of the system of equations and boundary conditions: $\beta = 5\cdot10^{-7}$, $\Pi = 10^{-3}$, $\eta = 8\cdot10^{-5}$, $E = 10^3$, $N_1 = 0{,}2$, $N_2 = 0{,}4$, $N_3 = 1$, $\delta = 10^{-4}$, $A_k = 1/n$, $B_k = 1$, $D_k = 1$, $v_0 = 0{,}1$. $\rho_0 = 1$, $v(0) = 0{,}1$, $\rho(0) = 1$. Analyzing the dependence of the magnetic induction in the channel (in Fig. 2 we have plotted lines of equal values of magnetic induction) on the number of RLC sections in the store, we see that with n = 1, at the beginning of the channel an increase in the magnetic induction is observed as the radius increases. Similar behavior is possible in the case of an electric eddy current in this part of the channel. As n is increased, the magnetic induction in the channel decreases, and the eddy currents are smoothed out. If when n = 1, at the instant of time $\tau = 2$ the current flows mainly in the beginning of the channel, as follows from the magnetic induction distribution, then as n increases a more uniform current distribution in the channel is observed. This current distribution also affects the variation in the remaining plasma parameters.

The variation in the current in the electric circuit with time for a different distribution of the elements in the store agrees qualitatively with the results obtained in [11].

The distribution of the plasma velocity in the channel is shown in Fig. 3. Here the arrows represent the direction of the velocity, and lines of equal velocity are shown. It is seen that the acceleration of the plasma at the instant of time considered when n = 1 occurs only in part of the channel. The maximum value of the

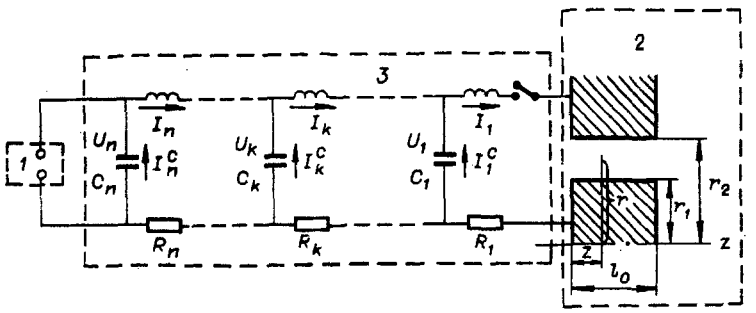

Fig. 1

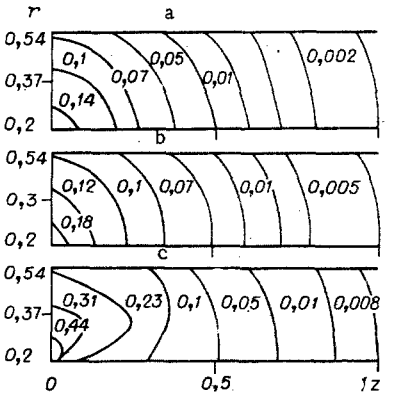

Fig. 2

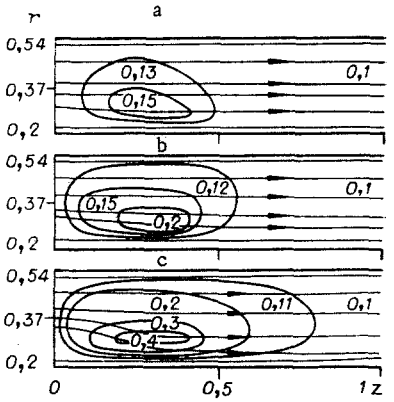

Fig. 3

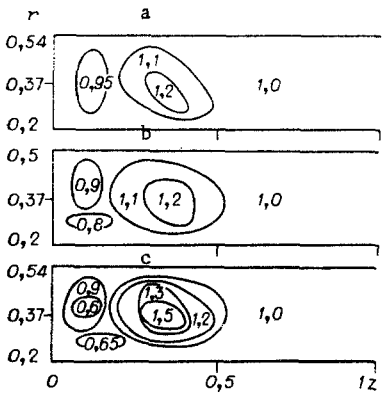

Fig. 4

velocity is approximately four times greater than the value of the velocity both at the input of the channel and at the output. As the number of RLC sections is increased (while keeping the capacitance and the energy of the capacitor battery constant), the value of the magnetic induction decreases at the input of the channel and the increment of velocity falls, although the velocity distribution pattern of the plasma in the channel remains similar to that in the case when $n = 1$. The reduction in the velocity increment when the number of RLC sections is increased does not indicate a reduction in the efficiency of the accelerating chamber, since as n increases, the duration of the discharge of the capacitor battery and, consequently, the time it acts on the plasma increase.

The variation in the plasma density in the channel for different values of n is shown in Fig. 4. It is seen that after a time interval $0 < \tau \leq 2$ the perturbation no longer propagates over the whole channel. The compression wave reaches only to the middle of the channel. After the wave of increased density there follows a zone of rarefaction. In this case the densities in the compression and rarefaction zones differ by a factor of

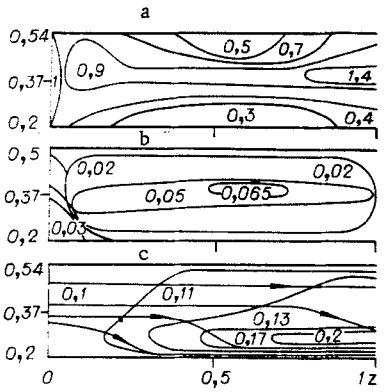

Fig. 5

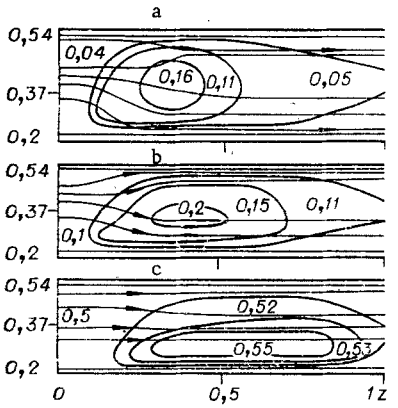

Fig. 6

approximately two for n = 1 and decreases as the number of RLC sections increases (with a reduction in the value of the magnetic induction at the input of the channel). The increase in the plasma density with a simultaneous increase in the velocity occurs due to the fact that the moving plasma layers enter the region of unperturbed plasma.

For illustration, Fig. 5a-c shows the variation in the density, magnetic inductions, and velocity in the channel, respectively, for the above-mentioned parameters with n = 11 at the instant of time $\tau = 7$. It is seen that plasma acceleration occurs over the whole volume of the channels. The maximum plasma velocity is at the putput. Before the instant considered on the electrodes there is a pronounced rarefaction zone and there is already a small region of the channel where plasma with increased density has not yet left.

The value of the magnetic induction in the channel is higher than at the input and the region with maximum magnetic induction is at the center of the channel. This variation of the magnetic field gives rise to eddy currents in the channel.

For other plasma velocities at the input to the channel and an unchanged distribution of the RLC sections in the energy store there is no qualitative change in the nature of the plasma flow. Figure 6 shows the variation in the plasma velocities in the channel for different plasma velocities at the input at the instant of time $\tau = 1.2$ for n = 1 and the following values of the dimensionless parameters: $\beta = 5 \cdot 10^{-3}$, $\Pi = 20$, $\eta = 8 \cdot 10^{-2}$, $E = 10^3$, $N_1 = 0{,}2$, $N_2 = 0{,}4$, $N_3 = 1$, $\delta = 1$, $\rho_0 = 1$, $\rho(0) = 1$. It is seen that a greater variation in the plasma velocity in the channel is observed for lower input velocities.

It follows from the above results that by varying the number of RLC sections in the capacitive energy store, one can vary the plasma flow pattern in the channels.

LITERATURE CITED

1. L. A. Artsimovich, S. Yu. Luk'yanov, I. M. Podgornyi, and S. A. Chubatin, "Electrodynamic acceleration of plasma bunches," Zh. Tekh. Fiz., 33, No. 1 (1957).

2. N. V. Belan, V. I. Kiryushko, and N. A. Mashtylev, "The current distribution in a coaxial accelerator," Zh. Tekh. Fiz., 40, No. 1 (1970).
3. A. A. Kalmykov, "Pulsed plasma accelerators," in: Physics and Applications of Plasma Accelerators [in Russian], Nauka i Tekhnika, Minsk (1974).
4. P.E. Kovrov and A. P. Shubin, "High-current coaxial accelerator in the quasistationary mode," in: Physics and Applications of Plasma Accelerators [in Russian], Nauka i Tekhnika, Minsk (1974).
5. K. V. Brushlinskii and A. I. Morozov, "Calculation of two-dimensional plasma flows in channels," in; Problems of Plasma Theory [in Russian], No. 8, Atomizdat, Moscow (1974).
6. K. V. Brushlinskii, A. I. Morozov, V.V. Paleichik, and V. V. Solov'ev, "Calculation of compression plasma flows in coaxial channels," Fiz. Plazmy, 2, No. 4 (1976).
7. N. V. Belan, S. I. Zabara, N. A. Mashtylev, and A. I. Morozov, "Calculation of the two-dimensional nonstationary isothermal plasma flow in a coaxial channel," in: Proceedings of the Second All-Union Conference on Plasma Accelerators, [in Russian], Minsk (1973).
8. N. V. Belan, N. A. Mashtylev, and L. V. Shushlyapin, "Two-dimensional motion of a heat-conducting plasma in a pulsed accelerator," in: Proccedings of the Second All-Union Conference on Plasma Accelerators, [in Russian], Minsk (1973).
9. N. V. Belan, N. A. Mashtylev, and S. I. Zabara, "Calculation of two-dimensional nonstationary plasma flow in coaxial channels," in: Low-Temperature Plasma Sources [in Russian], No. 1, Izd. KhAI, Khar'kov (1975).
10. I. S. Berezin and N. P. Zhidkov, Computational Methods [in Russian], Fizmatgiz, Moscow (1959).
11. N. V. Belan, N. A.Mashtylev, B. I. Panachevnyi, and L. V. Shushlyapin, "Effect of the distribution of the elements in a capacitive energy store on the form of the current in a pulsed plasma injector," Zh. Tekh. Fiz., 43, No. 6 (1974).

INVESTIGATION OF SLIDING SPARK IN AIR

S.I. Andreev, E. A. Zobov, and A. N. Sidorov

UDC 533.9+518.5+537.517

Sliding sparks occur on the surface of a dielectric under whose layer there is a conductor [1]. They appear especially easily if this conductor (we henceforth call it the initiator) is electrically connected to one of the electrodes.

Extensive literature (for instance, [1-8]) is devoted to the study of sliding sparks. Mainly the conditions for the origination of such discharges in high-voltage techniques have been studied. Questions on the dynamics of development have been investigated in [7, 8]. These investigations refer to the domain of comparatively small gaps ($l \leq 0.24$ m).

The present paper is devoted to an investigation of the physical processes for the development of sliding sparks from short to long (8 m) gaps.

METHODOLOGY OF THE EXPERIMENT

Sliding sparks occurred on the surface of thin-film dielectrics covered either with thin metal surfaces or tubes. A voltage being formed during the discharge of a condenser battery with $C = 0.5-16$ μF (Fig. 1a) through a controllable discharger 1 on the primary winding (one turn) of a cable transformer 2 was used in the research. A voltage in the form of a damped cosinusoid with a period of 2-18 μsec (a logarithmic damping decrement of ~0.01) occurred at the secondary winding (ten turns). This voltage was applied to the electrodes of the discharge gap (DG) under investigation. An oscillogram was made by using the divider D_0. The maximum value was determined by using a ball 3 of diameter 380 mm (the calibration tables were taken from [5]).

The current distribution was measured along the length of the channel (Fig. 1b). To do this, the initiator 4 was fabricated from mutually insulated flat metal plates. The current shunts Sh permitted taking oscill-

Leningrad. Translated from Zhurnal Prikladnoi Mekhaniki i Tekhnicheskoi Fiziki, No. 3, pp. 38-43, May-June, 1978. Original article submitted December 23, 1976.

0021-8944/78/1903-0309$07.50